MULTI–OBJECTIVE OPTIMIZATION OF TUNED MASS DAMPERS CONSIDERING SOIL–STRUCTURE INTERACTION

M. Khatibinia[*, †], H. Gholami and S.F. Labbafi
Department of Civil Engineering, University of Birjand, Birjand, Iran

ABSTRACT

Tuned mass dampers (TMDs) are as a efficient control tool in order to reduce undesired vibrations of tall buildings and large–span bridges against lateral loads such as wind and earthquake. Although many researchers has been widely investigated TMD systems due to its simplicity and application, the optimization of parameters and placement of TMD are challenging tasks. Furthermore, ignoring the effects of soil–structure interaction (SSI) may lead to unrealistic desig of structure and its dampers. Hence, the effects of SSI should be considered in the design of TMD. Therefore, the main aim of this study is to optimize parameters of TMD subjected to earthquake and considering the effects of SSI. In this regard, the parameters of TMD including mass, stiffness and damping optimization are considered as the variables of optimization. The maximum absolute displacement and acceleration of structure are also simultaneously selected as objective functions. The multi–objective particle swarm optimization (MOPSO) algorithm is adopted to find the optimal parameters of TMD. In this study, the Lagrangian method is utilized for obtaining the equations of motion for SSI system, and the time domain analysis is implemented based on Newmark method. In order to investigate the effects of SSI in the optimal design of TMD, a 40 storey shear building with a TMD subjected to the El–Centro earthquake is considered. The numerical results show that the SSI effects have the significant influence on the optimum parameters of TMD.

Keywords: tuned mass dampers; soil–structure interaction; displacement; acceleration; multi–objective particle swarm optimization algorithm.

1. INTRODUCTION

Due to flexibility and low damper ratio, tall buildings are highly susceptible to wind and

---

[*]Corresponding author: Department of Civil Engineering, University of Birjand, Birjand, Iran
[†]E-mail address: m.khatibinia@birjand.ac.ir (M. Khatibinia)

earthquake loads. By an appropriate design and under normal conditions, the response of the structure remains safe. However, when structure is exposed to earthquakes and strong winds, there is no guarantee that the structure has responses in safe area. For achieving this purpose, effective controlling devices are required in structures. Tuned mass dapmer (TMD) is one of the most reliable and conventional controlling device. A TMD system consists of a mass–spring–dashpot system attached to a primary structure [1]. The system dissipates the energy of vibration by the combined action of the inertial force caused by the movement of the mass, and the damping effect induced by this device.

In seismic design of strucrures, it is assumed that structures are fixed to their base, which may considered as a realistic hypothesis only when these are founded on relatively solid rock or very stiff soil. The seismic responses of a structure constructed on deformable soil may differ significantly compared to the fixed base a ssumption. In fact, the seismic excitation experienced by a structure is a function of local site effect and dynamic soil–structure interaction (SSI) influences. Thus, the SSI effects have important role in the seismic assessment and desing of structures constructed on relatively soft soil [2–4].

Several studies have highlighted the effects of elastic dynamic SSI on the structural response [5–8]. Xu and Kwak [9] investigated the wind–induced motion of tall/slender structures equipped with TMD considering SSI. A transfer matrix formulation was used to analyse the soil–structure–mass damper interaction in the frequency domain. The results of this study show that soil compliancy affect structural responses and the effectiveness of TMDs. Wu et al. [10] presented how SSI affects the seismic performance of TMDs installed on flexibly based structures. In this study, a generic frequency–independent model was used to represent a general soil–structure system, whose parameters cover a wide spectrum of soil and structural characteristics. Liu et al. [11] developed a mathematical model for predicting wind–induced oscillations of a high–rise building with a TMD considering the SSI effects. The results of this study indicated that this model can simulate the effects of soil well and it is much more accurate than the model with a fixed base.

Three main and effective parameters consisting of mass, damping and stiffness are considered in the design of TMDs. For the first time, the optimum design of parameters were considered by Den Hartog [12], where an undamped single degree of freedom (SDOF) system was subjected to the harmonic loading. Later, the main system with damping investigated by several researches. Using numerical searching technique, the optimum parameters of TMD system attached to a viscously damped single degree–of–freedom main system were derived for various combinations of excitation and response parameters [13]. Wang et al. [14] presented a two–stage optimum design procedure for passive tuned mass dampers (PTMDs) in order to reduce structural dynamic responses with the limitation of PTMD stroke. Marano et al. [15] introduced the optimum mass ratio of TMD which was considered as a preselected parameter in previous studies. Arfiadi and Hadi [16] utilized genetic algorithms in order to optimize the location and properties of TMD. In the study of Bekdas and Nigdeli [17], harmony search (HS) algorithm was employed as an optimization technique to find the optimum parameters of TMD subjected to harmonic loading. The results of this study show that the structural responses have a significant reduction, however, these results discussed by Miguel et al. [18] and Bekdas and Nigdeli [19]. Nigdeli and Bekdas [20] utilized HS in order to find the optimum parameters of TMD for preventing brittle fracture by reducing shear force. Farshidianfar and Soheili [21, 22] investigated the

optimal parameters of TMDs involving SSI effects. Althought, Rahai *et al.* [23] have recenlty demonstrated that the formulation of the SSI model proposed by Farshidianfar and Soheili [21, 22] is not accurate enough. Xiang and Nishitain [24] introduced the optimal design of a non–traditional TMD that is directly connected to the ground by a dashpot and adopted to mitigate the resonant behavior of a structure. Salvi and Rizzi [25] proposed the optimum tuning of the free parameters of a passive TMD applied to sample frame structures subjected to selected seismic excitations. In the work of Mohebbi *et al.* [26], the optimal design and assessment of multiple TMDs capability in mitigating the damage of nonlinear steel structures subjected to earthquake excitation were investigated. Recently, using charged system search method, Kaveh *et al.* [27] have investigated the optimum parameters of TMD under seismic excitations. Kaveh *et al.* [28] have also presented the efficacy of an optimized fuzzy controller for reducing the responses of a building structure with semi– active TMD under earthquake excitations.

   This study persents the optimal parameters of TMD subjected to earthquake considering the effects of SSI. In order to acheive this purpose, the parameters of TMD including mass, stiffness and damping optimization are considered as variables of optimization. Furthermore, the maximum absolute displacement and acceleration of structure are simultaneously adopted as objective functions in the framework of the multi–objective optimization problem. The multi–objective particle swarm optimization (MOPSO) algorithm is selected to find the optimal parameters of TMD. In this study, the Lagrangian method [29] is utilized for obtaining the equations of motion for SSI system. To solve this equations of motion, the time domain analysis based on the Newmark method is employed. In order to show the effects of SSI in the optimal design of the TMD parameters, the optimal parameters of TMD for a 40 storey shear building subjected to the El–Centro earthquake are investigated with and without the SSI effects. The optimum results demonstrate that the SSI effects have the significant influence on the optimum parameters of TMD and should be considered in the optimal design of TMD system.

2. MULTI–OBJECTIVE OPTIMIZATION PROBLEM OF TMD

The main aim of this study is to optimize the parameters of a TMD system subjected to earthquake excitation considering the SSI effects. In order to achieve this purpose, the optimal parameters of TMD in terms of the damping mass, coefficient and spring stiffness are determined through simultaneously minimizing the maximum absolute acceleration and displacement of structure. Thus, the optimal design of a TMD system in a *n* degree–of– freedom structure can be formulated as:

$$
\begin{aligned}
&\text{Find}: \quad M_{TMD}, K_{TMD}, C_{TMD} \\
&\text{Minimize}: \ \max(|x_i(t)|) \text{ and } \max(|a_i(t)|) \ ; \quad t=1,2,\ldots,t_{max} \ , \quad i=1,2,\ldots,N
\end{aligned}
\tag{1}
$$

where M_{TMD}, K_{TMD} and C_{TMD} are stiffness, mass and damper of TMD, respectively. $x_i(t)$ and $a_i(t)$ are the displacement and acceleration of *i*th storey at the *t*th time, respectively. Furthermore, *N* is the number of structure storeris.

3. MODELLING OF SOIL – STRUCTURE INTERACTION SYSTEM WITH TMD

In this section, a theoretical model is developed for calculating the earthquake–induced vibration of a storey shear building with a TMD and considering the SSI effects. The structural responses of structure are calculated in time domain. In order to achieve this purpose, the systems of structure and its subsoil are considered respectively as shear building system and spring. In Fig. 1, a N–shear structure model with TMD and its subsoil model is displayed. M_i, C_i, K_i, and X_i represent, respectively the mass, damping, stiffness and the displacement for the ith storey. M_{TMD}, C_{TMD}, K_{TMD} are the corresponding parameters of the TMD. M_0 and I_0 are defined, respectively as mass and mass moment of inertia of the foundation. C_s and C_r represent dampings of the swaying and the rocking dashpots, and K_s and K_r denote stiffness of the corresponding springs of soil.
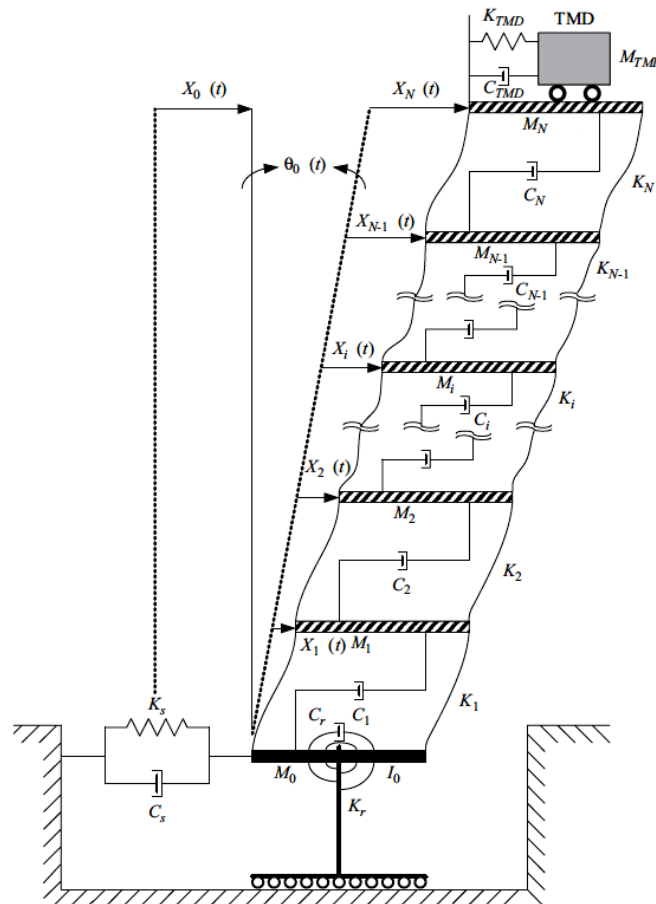

Figure 1. Geometrical model of the SSI system

In this study, the Lagrangian method [29] is utilized in order to develop the equations of motion for the SSI system. In the Lagrange method, first, the kinetic and potential energy of the SSI system are obtained. Equtions (2) and (3) representes the kinetic and potential

energy of the SSI system in the generalized coordinates, respectively:

$$T = \frac{1}{2}M_0\dot{u}^2 + \frac{1}{2}I_0\dot{\theta}^2 + \frac{1}{2}M_1(\dot{u}+Z_1\dot{\theta}+\dot{X}_1)^2 + \frac{1}{2}I_1\dot{\theta}^2 + \frac{1}{2}M_2(\dot{u}+Z_2\dot{\theta}+\dot{X}_2)^2 + \frac{1}{2}I_2\dot{\theta}^2 + \cdots +$$
$$\frac{1}{2}M_{N-1}(\dot{u}+Z_{N-1}\dot{\theta}+\dot{X}_{N-1})^2 + \frac{1}{2}I_{N-1}\dot{\theta}^2 + \frac{1}{2}M_N(\dot{u}+Z_N\dot{\theta}+\dot{X}_N)^2 + \frac{1}{2}I_N\dot{\theta}^2 + \frac{1}{2}M_{TMD}(\dot{u}+Z_N\dot{\theta}+\dot{X}_{N+1})^2 \quad (2)$$

$$U = \frac{1}{2}K_s u^2 + \frac{1}{2}K_r\dot{\theta}^2 + \frac{1}{2}K_1 X_1^2 + \frac{1}{2}K_2(X_2-X_1)^2 + \cdots + \frac{1}{2}K_{N-1}(X_{N-1}-X_{N-2})^2 \quad (3)$$
$$+ \frac{1}{2}K_N(X_N - X_{N-1})^2 + \frac{1}{2}K_{TMD}(X_{N+1}-X_N)^2$$

Then, using the derivatives of the kinetic and potential energy respect to each of the generalized coordinates, the equations of motion for the SSI system are obtained as follows:

$$[\mathbf{M}]\{\ddot{X}(t)\} + [\mathbf{C}]\{\dot{X}(t)\} + [\mathbf{K}]\{X(t)\} = -\left[\mathbf{m}^*\right]\{\mathbf{I}\}\ddot{u}_g(t) \quad (4)$$

where $[\mathbf{M}]$, $[\mathbf{C}]$ and $[\mathbf{K}]$ are the mass, damping, and stiffness of the SSI system, respectively. $[\mathbf{m}^*]$ indicates acceleration mass matrix for earthquake; and $\ddot{u}_g(t)$ is the earthquake acceleration.

By considering N degrees of freedom for structure, the number of freedom degrees for the effects of SSI system is $N+3$. The mass matrix in Eq. (4) can be obtained based on the following equations:

$$[\mathbf{M}] = \begin{bmatrix} [\mathbf{M}]_{N\times N} & \{\mathbf{0}\}_{N\times 1} & [\mathbf{M}]_{N\times 1} & [\mathbf{MZ}]_{N\times 1} \\ & M_{TMD} & M_{TMD} & M_{TMD}Z_N \\ & & M_0 + \sum\limits_{j=1}^{N} M_j + M_{TMD} & \sum\limits_{j=1}^{N} M_j Z_j + M_{TMD}Z_N \\ sym & & & I_0 + \sum\limits_{j=1}^{N}(I_j + M_j Z_j^2) + M_{TMD}Z_N^2 \end{bmatrix} \quad (5)$$

$$[\mathbf{M}]_{N\times N} = \begin{bmatrix} M_1 & 0 & 0 & 0 & 0 \\ & M_2 & 0 & 0 & 0 \\ & & \cdots & \{0\} & \{0\} \\ & & & M_{N-1} & 0 \\ sym & & & & M_N \end{bmatrix} \quad (6)$$

$$\{\mathbf{M}\}_{N\times 1} = \begin{Bmatrix} M_1 \\ M_2 \\ \vdots \\ M_N \end{Bmatrix} \; ; \; \{\mathbf{MZ}\}_{N\times 1} = \begin{Bmatrix} M_1 Z_1 \\ M_2 Z_2 \\ \vdots \\ M_N Z_N \end{Bmatrix} \quad (7)$$

The damping matrix is expressed as following:

$$[\mathbf{C}] = \begin{bmatrix} [\mathbf{C}]_{(N+1)\times(N+1)} & \{\mathbf{0}\}_{(N+1)\times1} & \{\mathbf{0}\}_{(N+1)\times1} \\ & C_s & 0 \\ sym & & C_r \end{bmatrix} \tag{8}$$

In addition, the stiffness matrix is achieved using following equations:

$$[\mathbf{K}] = \begin{bmatrix} [\mathbf{K}]_{(N+1)\times(N+1)} & \{\mathbf{0}\}_{(N+1)\times1} & \{\mathbf{0}\}_{(N+1)\times1} \\ & K_s & 0 \\ sym & & K_r \end{bmatrix} \tag{9}$$

$$[\mathbf{K}]_{(N+1)\times(N+1)} = \begin{bmatrix} K_1 + K_2 & -K_2 & 0 & 0 & 0 \\ & K_2 + K_3 & 0 & 0 & 0 \\ & & \cdots & \vdots & \{0\} \\ & & & K_N + K_{TMD} & -K_{TMD} \\ sym & & & -K_{TMD} & K_{TMD} \end{bmatrix} \tag{10}$$

Finally, the acceleration mass is as follows:

$$\begin{bmatrix} \mathbf{m}^* \end{bmatrix} = \begin{bmatrix} [\mathbf{M}]_{N\times N} & \{\mathbf{0}\}_{N\times1} & \{\mathbf{0}\}_{N\times1} & \{\mathbf{0}\}_{N\times1} \\ 0 & M_{TMD} & 0 & 0 \\ 0 & 0 & M_0 + \sum_{j=1}^{N} M_j + M_{TMD} & 0 \\ 0 & 0 & \sum_{j=1}^{N} M_j Z_j + M_{TMD} Z_N & 0 \end{bmatrix} \tag{11}$$

The damping matrix can be obtained using the Rayleigh method [29], as follows:

$$\begin{bmatrix} \mathbf{C} \end{bmatrix}_{N\times N} = A_0 \begin{bmatrix} \mathbf{M} \end{bmatrix}_{N\times N} + A_1 \begin{bmatrix} \mathbf{K} \end{bmatrix}_{N\times N} \tag{12}$$

where A_0 and A_1 are the Rayleigh damping ratios.

Fethermore, the vector $X(t)$ includes also displacement and foundation rotation defined as follows:

$$X(t) = \{X_1(t), X_2(t), \ldots, X_N(t), X_{TMD}(t), X_0(t), \theta_0(t)\}^T \tag{13}$$

In this study, the Newmark method [29] is utilized in order to solve the motion equations of SSI system.

4. MULTI–OBJECTIVE PARTICLE SWARM OPTIMIZATION

Let $S \subset \Re^n$ be an n–dimensional search space, and $\vec{f}_i(\bar{X}), i = 1, 2, \ldots, k$ be k objective functions which are defined over S. Also let f be a vector function defined as, $f(\bar{X}) = \{f_1(\bar{X}), f_2(\bar{X}), \ldots, f_k(\bar{X})\}$. Then, the goal of multi–objective optimization is to find a solution, $\bar{X} = \{\bar{x}_1, \bar{x}_2, \ldots, \bar{x}_n\}$, that minimizes $f(\bar{X})$. However, a multi–objective problem, in principle, produces a set of optimal solutions known as Pareto–optimal solutions instead of a single optimal solution. Each point in the Pareto optimal solution set is optimal in the sense that improvement in one objective function leads to degradation in at least one of the remaining objective functions.

Solving multi-objective optimization problems is still a challenge. The performance of different multi-objective algorithms has been tested in the work of Coello *et al.* [30] The results of this study have been shown that Multi–objective Particle Swarm Optimization (MOPSO) [30] is the best in covering the full Pareto front of all the functions used in their study. In addition, it has been found to converge with a low computational time. Hence, in this study the MOPSO method is selected to find the optimal parameters of the TMD system.

4.1 The PSO method

In order to introduce MOPSO, a review of Particle Swarm Optimization (PSO) algorithm is expressed. The PSO algorithm as a meta–heuristic optimization technique has been inspired by the social behavior of animals such as fish schooling, insects swarming and birds flocking. The standard PSO was introduced by Kennedy and Eberhart [32] in the mid 1990s, while attempting to simulate the graceful motion of bird swarms as a part of a socio–cognitive study. It involves a number of particles, which are initialized randomly in the search space of an objective function. These particles are referred to as swarm. Each particle of the swarm represents a potential solution of the optimization problem.

The ith particle in tth iteration is associated with a position vector, $\bar{X}_i^t$, and a velocity vector, $\bar{V}_i^t$, that shown as following:

$$\bar{X}_i^t = \{\bar{x}_{i1}^t, \bar{x}_{i2}^t, \ldots, \bar{x}_{in}^t\}$$
$$\bar{V}_i^t = \{\bar{v}_{i1}^t, \bar{v}_{i2}^t, \ldots, \bar{v}_{in}^t\} \tag{14}$$

The particle fly through the solution space and its position is updated based on its velocity, the best position particle (***pbest***) and the global best position (***gbest***) that swarm has visited since the first iteration as:

$$\bar{V}_i^{t+1} = \omega^t \bar{V}_i^t + c_1 r_1 (\textbf{\textit{pbest}}_i^t - \bar{X}_i^t) + c_2 r_2 (\textbf{\textit{gbest}}^t - \bar{X}_i^t) \tag{15}$$
$$\bar{X}_i^{t+1} = \bar{X}_i^t + \bar{V}_i^{t+1} \tag{16}$$

where r_1 and r_2 are two uniform random sequences generated from interval [0, 1]; c_1 and c_2 are the cognitive and social scaling parameters, respectively; and ω^t is the inertia weight

used to discount the previous velocity of particle preserved.

It has been proposed that the cognitive and social scaling parameters c_1 and c_2 to be selected such that $c_1=c_2=2$ to allow the product $c_1 r_1$ or $c_2 r_2$ to have a mean of 1 [32]. One of the main parameters affecting the performance of PSO is the inertia weight, ω, in achieving efficient search behaviour. In this study, a dynamic variation of inertia weight proposed by linearly decreasing the inertia weight with each iteration algorithm [33] is utilized, as

$$\omega = \omega_{\max} - \frac{\omega_{\max} - \omega_{\min}}{t_{\max}} t \qquad (17)$$

where $\omega_{\max}$ and $\omega_{\min}$ are the maximum and minimum values of ω, respectively. Also, t_{max} is the numbers of maximum iteration. It is noted that the linearly decreasing inertia weight of PSO has provided the better balance between the global search and local search [32].

4.2 The MOPSO method

In multi–objective optimization problem, the objectives are normally in conflict to each other, which means that there is no single solution for these problems. Instead, the aim of the MOPSO algorithm is to find good tradeoff solutions that represent the best possible compromises among the objectives based on the concept of Pareto optimality [31]. A point $\bar{X}^* \subset \Omega$ is Pareto optimality if for every $\bar{X} \subset \Omega$ and $I = \{1, 2, \ldots, k\}$ either

$$\forall_{i \subset I} (f_i(\bar{X}) = f_i(\bar{X}^*)) \qquad (18)$$

or, there is at least one $i \subset I$ such that

$$f_i(\bar{X}) > f_i(\bar{X}^*)) \qquad (19)$$

It is defined that $\bar{X}^*$ is Pareto optimal if there exists no feasible vector $\bar{X}$ which would decrease some criterion without causing a simultaneous increase in at least one other criterion. In MOPSO, all objective functions are evaluated for each particle. Pareto optimality can guide the particles to produce non–dominated best positions (often called leaders). Since there can be many non–dominated solutions in the neighborhood of particle, the determination of leaders is not straightforward, but only one is usually selected to participate in the velocity update in PSO. The external archive is utilized for storing the non–dominated solutions discovered during search [34]. An external archive has bounded size, thereby making unavoidable the imposition of the rules regarding the replacement of existing solutions with new ones.

For solving the optimization problem of TMD considering the SSI effects The framework of the MOPSO method is depicted in Fig. 2.
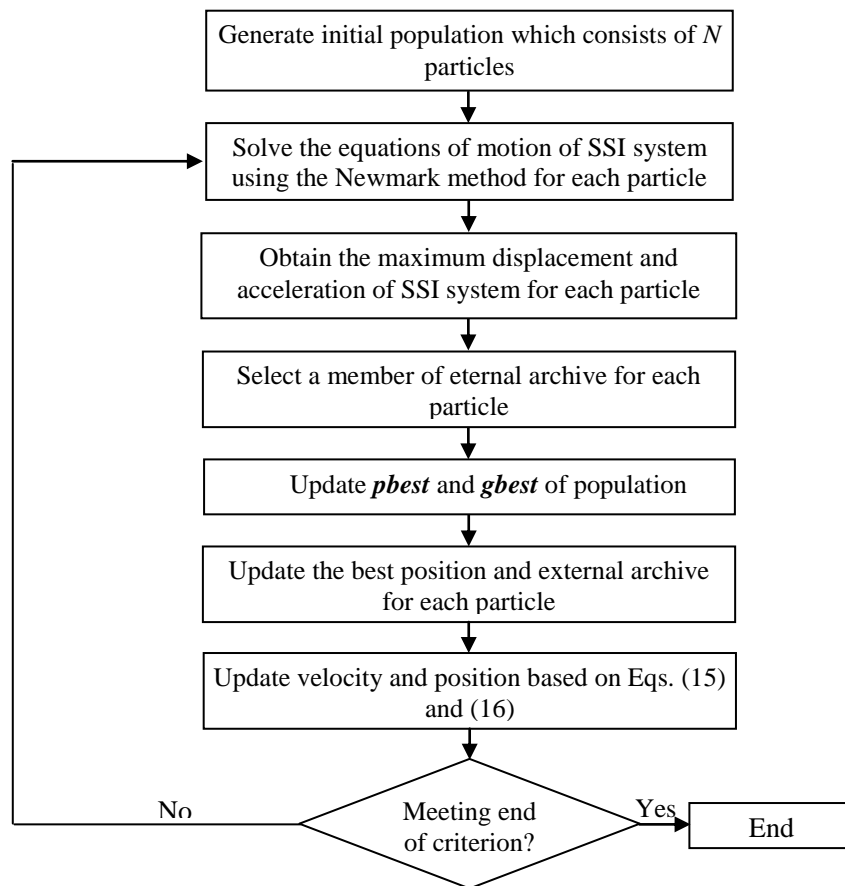
Figure 2. Flowchart of MOPSO for the optimal design of TMD considering the SSI effects

5. ILLUSTRATIVE EXAMPLE

In order to investigate the effects of SSI in the optimal design of the TMD parameters, a 40–storey shear structure with a TMD installed on the top of building is chosen. This structure has been studined in the works of Farshidianfar and Soheili [21, 22]. Table 1 shows the properties of the structure. In this study, foundation is assumed to be on two types of soil, namely soft and medium soil. The properties of soil and foundation are also presented in Table 2.

Table 1: The parameters of the structure [21]

Parameter	Value
Height of storey (m)	4
Mass of storey (kg)	9.8×10^5
Inertia moment of storey ($kg.m^2$)	1.31×10^8
Stiffness of storey (N/m)	$K_1 = 2.31 \times 10^9 - K_{40} = 9.98 \times 10^8$
Mass of foundation (kg)	1.96×10^6
Inertia moment of foundation ($kg.m^2$)	1.96×10^8

Table 2: Soil and foundation parameters [21]

Type of soil	$K_r(N.s/m)$	$K_s(N.s/m)$	$C_r(N/m)$	$C_s(N.s/m)$
Soft	7.53×10^{11}	1.91×10^9	2.26×10^{10}	2.19×10^8
Medium	7.02×10^{12}	1.8×10^{10}	7.02×10^{10}	6.9×10^8

The lower and upper bounds of the TMD parameters defined in Section (2) are shown in Table 3:

Table 3: Upper and lower bands of TMD parameters [21]

Parameter of TMD	Lower bound	Upper bound
$M_{TMD}(kg)$	100×10^3	2000×10^3
$C_{TMD}(N.s/m)$	0.1×10^3	2000×10^3
$K_{TMD}(N/m)$	0.5×10^6	60×10^6

The optimal design of the TMD parameters is found for the SSI system subjected to the El–Centro earthquake. This component of the recorded ground motion is shown in Fig. 3.
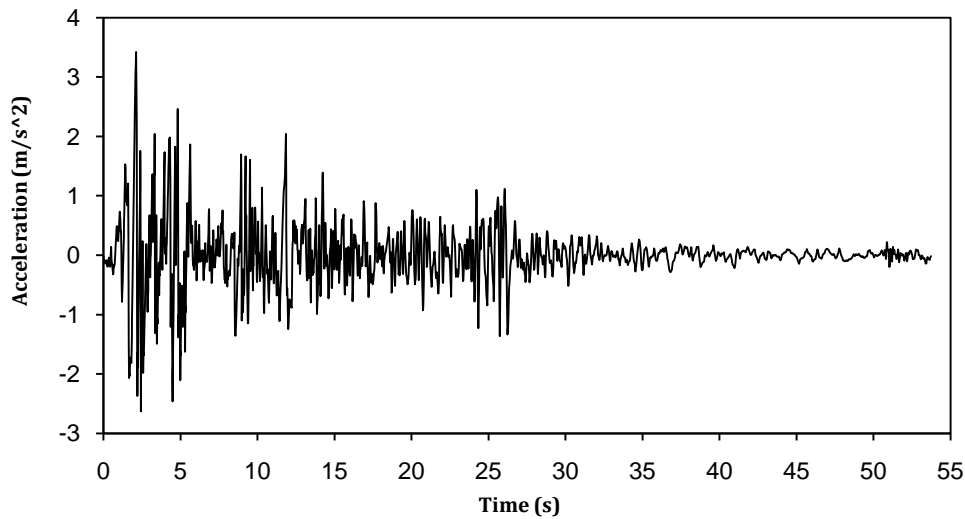

Figure 3. Accelerogram of the El–Centro earthquake

The parameters of the MOPSO algorithm are the following: the initial inertia weight $\omega_{max}=0.95$ and the final inertia weight $\omega_{min}=0.4$. Furthermore, a random initial population of 50 individuals is created for each of this runs. A size of 50 is adopted for the external repository. To demonstrate the SSI effect in the optimal design of the TMD parameters, two cases of optimization are considered and compared as follows:

Case 1: The optimal design of the TMD parameters for building in the fixed base (without SSI effects).

Case 2: The optimal design of the TMD parameters for building in the flexible base (with SSI effects).

6. OPTIMIZATION RESULTS AND DISCUSSIONS

In order to consider the stochastic nature of the MOPSO process, ten independent optimization runs are performed for each case, and three Pareto fronts are selected and reported in Tables 4 to 6.

Table 4: Optimal values of the TMD parameters and the maximum responses of the structure for three selected Pareto fronts in the case 1

Selected Pareto front	$M_{TMD}(kg)$	$C_{TMD}(N.s/m)$	$K_{TMD}(N/m)$	Maximum acceleration (m/s^2)	Maximum displacement (m)
1	1672.839×10^3	950.012×10^3	2927.723×10^3	5.130	0.264
2	1011.311×10^3	551.251×10^3	1358.793×10^3	5.129	0.276
3	426.946×10^3	100	60000×10^3	5.122	0.286

Table 5: Optimal values of the TMD parameters and the maximum responses of the structure for three selected Pareto fronts in the case 2 (soft soil)

Selected Pareto front	$M_{TMD}(kg)$	$C_{TMD}(N.s/m)$	$K_{TMD}(N/m)$	Maximum acceleration (m/s^2)	Maximum displacement (m)
1	285.327×10^3	1264.755×10^3	54845.863×10^3	4.317	0.232
2	1528.153×10^3	100	500×10^3	4.322	0.189
3	1546.244×10^3	180.486×10^3	1665.521×10^3	4.324	0.100

Table 6: Optimal values of the TMD parameters and the maximum responses of the structure for three selected Pareto fronts in the case 2 (medium soil)

Selected Pareto front	$M_{TMD}(kg)$	$C_{TMD}(N.s/m)$	$K_{TMD}(N/m)$	Maximum acceleration (m/s^2)	Maximum displacement (m)
1	1990.553×10^3	17.628×10^3	45867.273×10^3	5.291	0.199
2	1955.066×10^3	104.151×10^3	3558.901×10^3	5.273	0.222
3	1832.229×10^3	232.115×10^3	543.141×10^3	5.270	0.242

As can be observed from the optimal design of the TMD parameters shown in Tables 4–6, the SSI effects have the significant influence on the optimum parameters of TMD. Hence, structural engineer should consider the SSI effects in the optimal design of TMD system. For the two cases, pareto optimal frontier for displacement and acceleration is depicted in Figs. 4-6.

For a Pareto front of each case shown Table 7, the time history displacement of the top storey of structure with and without TMD are plotted and compared in Figs. 7 to 9.
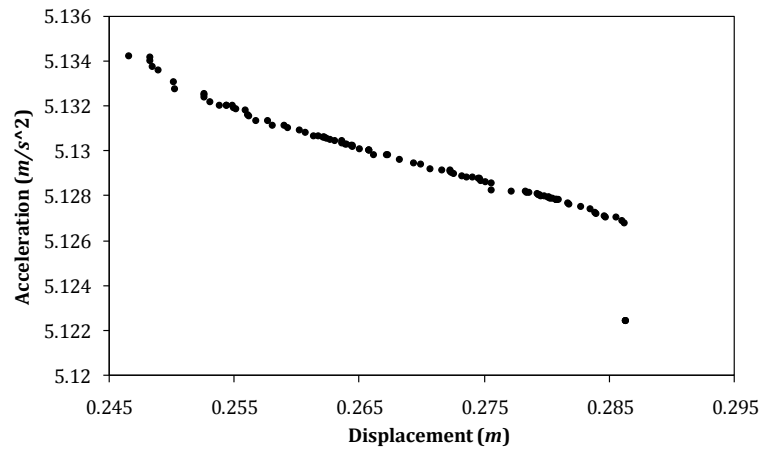
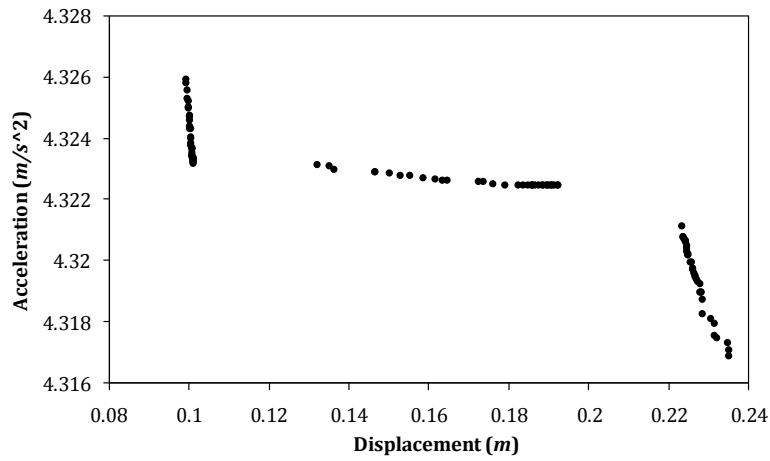Figure 4. Pareto optimal frontier for the case 1

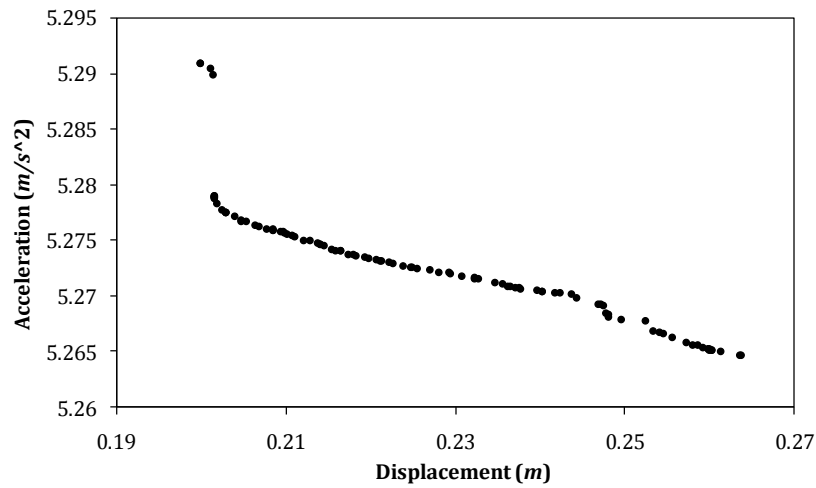Figure 5. Pareto optimal frontier for the case 2 (soft soil)

Figure 6. Pareto optimal frontier for with the case 2 (medium soil)

Table 7. Optimal values of the TMD parameters and the maximum structure responses for a selected Pareto front

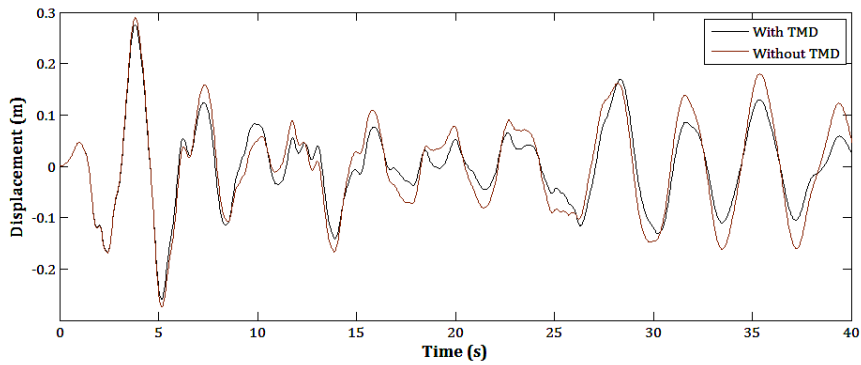| Case	$M_{TMD}\,(kg)$	$C_{TMD}\,(N.s/m)$	$K_{TMD}\,(N/m)$	Maximum acceleration (m/s^2)	Maximum displacement (m)
Without soil	1011.311×10^3	551.251×10^3	1358.793×10^3	5.129	0.276
Medium soil	1832.229×10^3	232.115×10^3	543.141×10^3	5.270	0.242
Soft soil	1546.244×10^3	180.486×10^3	1665.521×10^3	4.324	0.100

Figure 7. Time history displacement of the top storey for fixed case (without SSI)
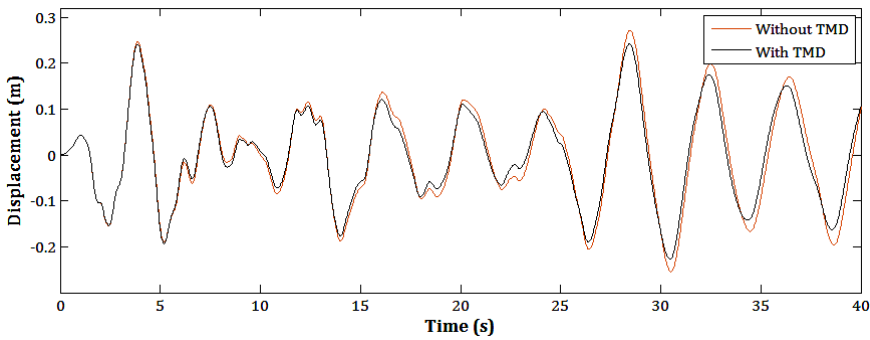

Figure 8. Time history displacement of the top storey for medium soil
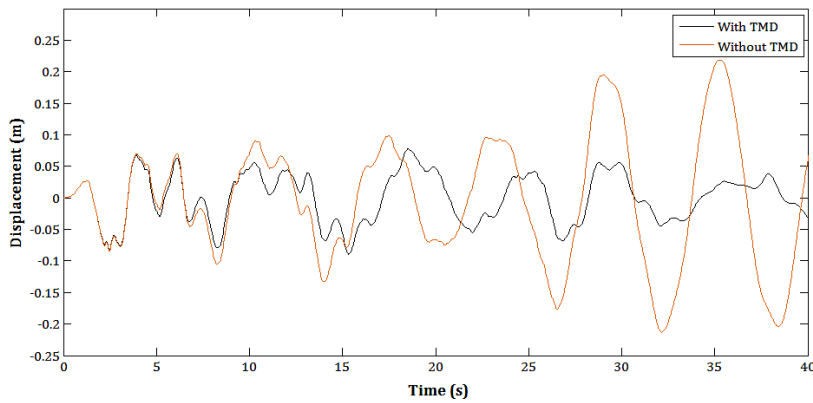

Figure 9. Time history displacement of the top storey for soft soil

It can be seen from Figs. 7 to 9 that the TMD system in comparison with uncontrolled structure decreases the displacement of sructure.

9. CONCLUSIONS

An efficient multi–objective optimization procedure is introduced to find the optimal parameters of a TMD system considering the effects of soil–structure interaction (SSI) for earthquake loading. In the optimization process, the parameters of TMD including mass, stiffness and damping optimization are considered as the variables of optimization. The maximum absolute displacement and acceleration of structure are also simultaneously adopted as objective functions. In order to achieve this purpose, the multi–objective particle swarm optimization (MOPSO) algorithm is utilized to find the optimal parameters of TMD. In this study, the equations of motion for SSI system is obtained based on the Lagrangian method.

The optimal results reveal that the SSI greatly influence on the TMD parameters. It is also indicated that the soil type also severely affects the time response of structures and the TMD parameters. Therefore, the SSI effects have an important role in the optimal design of TMD for structures constructed on relatively soft soil.

REFERENCES

1. Soong TT, Dargush GF. *Passive Energy Dissipation Systems in Structural Engineering*, John Wiley, Chichester, 1997.
2. Khatibinia M, Fadaee MJ, Salajegheh J, Salajegheh E. Seismic reliability assessment of RC structures including soil–structure interaction using wavelet weighted least squares support vector machine, *Reliab Eng Syst Safe* 2013; **110**: 22-33.
3. Khatibinia M, Salajegheh E, Salajegheh J, Fadaee MJ. Reliability–based design optimization of RC structures including soil - structure interaction using a discrete gravitational search algorithm and a proposed metamodel, *Eng Optimi* 2013; **45**(10): 1147-65.
4. Khatibinia M, Gharehbagh S, Moustafa A. *Seismic Reliability–Based Design Optimization of Reinforced Concrete Structures Including Soil–Structure Interaction Effects*, In book: Earthquake Engineering–From Engineering Seismology to Optimal Seismic Design of Engineering Structures, Publisher: In Tech, Editors: Abbas Moustafa, 2015; pp. 267-304.
5. Ghosh A, Basu B. Effect of soil interaction on the performance of tuned mass dampers for seismic applications, *J Sound Vib* 2004; **274**(3): 1079-90.
6. Wang JF, Lin CC. Seismic performance of multiple tuned mass dampers for soil irregular building interaction systems, *Int J Solids Struct* 2005; **42**(20): 5536-54.
7. Li C, Han B. Effect of dominant ground frequency and soil on multiple tuned mass dampers, *Struct Des Tall Spec Build* 2011; **20**(2): 151-63.

8. Li C. Effectiveness of active multiple-tuned mass dampers for asymmetric structures considering soil–structure interaction effects, *Struct Des Tall Spec Build* 2012; **21**(8): 543-65.
9. Xu YL, Kwok KC. Wind–induced response of soil–structure–damper systems, *J Wind Eng Ind Aerod* 1992; **43**(1): 2057-68.
10. Wu J, Chen G, Lou M. Seismic effectiveness of tuned mass dampers considering soil-structure interaction, *Earthq Eng Struct Dyn* 1999; **28**(11): 1219-33.
11. Liu MY, Chiang WL, Hwang JH, Chu CR. Wind–induced vibration of high–rise building with tuned mass damper including soil–structure interaction, *J Wind Eng Ind Aerod*, 2008; **96**(6): 1092-102.
12. Den Hartog JP. *Mechanical Vibrations*, McGraw–Hill, New York, 1959.
13. Bakre SV, Jangid RS. Optimal parameters of tuned mass damper for damped main system, *Struct Control Hlth* 2007; **14**(3): 448-70.
14. Wang JF, Lin CC, Lian CH. Two–stage optimum design of tuned mass dampers with consideration of stroke, *Struct Control Hlth* 2009; **16**(1): 55-72.
15. Marano GC, Greco R, Chiaia B. A comparison between different optimization criteria for tuned mass dampers design, *J Sound Vib* 2010; **329**(23): 4880-90.
16. Arfiadi Y, Hadi MN. Optimum placement and properties of tuned mass dampers using hybrid genetic algorithms, *Int J Optim Civil Eng* 2011; **1**(1): 167-87.
17. Bekdas G, Nigdeli SM. Estimating optimum parameters of tuned mass dampers using harmony search, *Eng Struct* 2011; **33**(9): 2716-23.
18. Miguel LFF, Lopez RH, Miguel LFF. Discussion of paper: Estimating optimum parameters of tuned mass dampers using harmony search, *Eng Struct* 2013: **54**: 262-64.
19. Bekdas G, Nigdeli SM. Response of discussion of paper: Estimating optimum parameters of tuned mass dampers using harmony search, *Eng Struct* 2013; **54**: 265-67.
20. Nigdeli SM, Bekdas G. Optimum tuned mass damper design for preventing brittle fracture of RC buildings, *Smart Struct Syst* 2013; **12**(2): 137-55.
21. Farshidianfar A, Soheili S. Ant colony optimization of tuned mass dampers for earthquake oscillations of high–rise structures including soil–structure interaction, *Soil Dyn Earthq Eng* 2013; **51**: 14-22.
22. Farshidianfar A, Soheili S. Optimization of TMD parameters for Earthquake Vibrations of Tall Buildings Including Soil Structure Interaction, *Int J Optim Civil Eng* 2013, **3**(3): 409-29.
23. Rahai AR, Saberi H, Saberi H. Discussion of paper: Ant colony optimization of tuned mass dampers for earthquake oscillations of high–rise structures including soil–structure interaction, *Soil Dyn Earthq Eng* 2016, In press.
24. Xiang P, Nishitani A. Optimum design for more effective tuned mass damper system and its application to base–isolated buildings, *Struct Control Hlth* 2014; **21**(1): 98–114.
25. Salvi J, Rizzi E. Optimum tuning of Tuned Mass Dampers for frame structures under earthquake excitation, *Struct Control Hlth* 2014; **22**(4): 707–25.
26. Mohebbi M, Moradpour S, Ghanbarpour. Improving the seismic behavior of nonlinear steel structures using optimal MTDs, *Int J Optim Civil Eng* 2014, **4**(1): 137-50.
27. Kaveh A, Mohammadi O, Khadem H, Keyhani A, Kalatjari VR. Optimum parameters of Tuned mass dampers for seismic applications using charged system search, *IJST T Civil Eng* 2015, **39**: 21-40.

28. Kaveh A, Pirgholizadeh S, Hosseini OK. Semi–active tuned mass damper performance with optimized fuzzy controller using CSS algorithm, *Asian J Civil Eng* 2015; **16**(5): 587-606.

29. Thomson W. *Theory of vibration with applications*, CRC Press, 1996.

30. Coello CAC, Pulido GT, Lechuga MS. Handling multiple objectives with particle swarm optimization, *IEEE Trans Evol Comput* 2004; **8**: 256-79.

31. Coello CA, Lechuga MS. MOPSO: A proposal for multiple objective particle swarm optimization*, Proceedings of the 2002 IEEE Congress of Evolutionary Computation* 2002; **2**: pp. 1051-60.

32. Kennedy J, Eberhart RC, Shi Y. *Swarm Intelligence*, Morgan Kaufmann Publishers, San Francisco, CA, 2001.

33. Shi Y, Liu H, Gao L, Zhang G. Cellular particle swarm optimization. *Inform Sci* 2011; **181**(20): 4460-93.

34. Baumgartner U, Magele C, Renhart W. Pareto optimality and particle swarm optimization, *IEEE T Magn* 2004; **40**(2): 1172-75.